J. Phys.: Condens. Matter **20** (2008) 325230 (7pp) doi:10.1088/0953-8984/20/32/325230

# Magnetization and $^{61}$Ni Mössbauer effect study of the ternary arsenide CrNiAs

**Z M Stadnik[1,4], P Wang[1], N Jansen[2], D Walcher[2], P Gütlich[2] and T Kanomata[3]**

[1] Department of Physics, University of Ottawa, Ottawa, ON, K1N 6N5, Canada
[2] Institut für Anorganische Chemie und Analytische Chemie, Johannes Gutenberg Universität, 55099 Mainz, Germany
[3] Faculty of Engineering Tohoku Gakuin University, Tagajo, Miyagi 985-8537, Japan

E-mail: stadnik@uottawa.ca

Received 1 May 2008
Published 18 July 2008
Online at stacks.iop.org/JPhysCM/20/325230

**Abstract**

The results of x-ray diffraction, dc magnetization, and $^{61}$Ni Mössbauer spectroscopy studies of the ternary arsenide CrNiAs are reported. This compound crystallizes in the orthorhombic $Fe_2P$-type structure (space group $P\bar{6}2m$) with the lattice parameters $a = 6.1128(2)$ Å and $c = 3.6585(1)$ Å. CrNiAs is a mean-field ferromagnet with Curie temperature $T_C = 171.9(1)$ K and the critical exponents $\beta = 0.514(18)$, $\gamma = 1.010(16)$, and $\delta = 2.922(10)$. The temperature dependence of the magnetic susceptibility above $T_C$ follows the modified Curie–Weiss law with a paramagnetic Curie temperature of 176.0(3) K and effective magnetic moment per transition metal atom of 2.42(1) $\mu_B$. The magnetic moment per formula unit at 4.2 K is found to be 1.114(33) $\mu_B$. The hyperfine magnetic field at $^{61}$Ni nuclei at 4.2 K of 41.5(1.0) kOe implies that the Ni atoms carry a magnetic moment of 0.15(3) $\mu_B$, and that the moment carried by the Cr atoms is 0.95(6) $\mu_B$. The Debye temperature of CrNiAs is 221(1) K.

(Some figures in this article are in colour only in the electronic version)

## 1. Introduction

The ternary transition-metal arsenides $(T_{1-x}T'_x)_2As$ (T, T′ = transition metal) have been investigated intensively with respect to their crystal structures and greatly varying physical properties [1–26]. These compounds crystallize either in the hexagonal $Fe_2P$-type structure or in the orthorhombic $Co_2P$-type structure. Common to these two structure types is a sub-cell where there are two kinds of transition-metal sites: the tetrahedral site surrounded by four As atoms and the pyramidal site surrounded by five As atoms. The arsenides $(T_{1-x}T'_x)_2As$ show almost all possible types of magnetic ordering: ferromagnetism, antiferromagnetism, ferrimagnetism, and spin glass. The ternary arsenides containing Ni, $(Cr_{1-x}Ni_x)_2As$ [10], are ferromagnetic for $0.45 < x \leqslant 0.7$ and antiferromagnetic for $0.4 < x \leqslant 0.45$.

The ternary arsenide CrNiAs is a ferromagnet with the Curie temperature, $T_C$, reported to be in the range of 182–195 K [1, 6, 10, 12, 22, 25] and the magnetic moment per formula unit, $\mu_{FU}$, reported to be in the range of 1.10–1.19 $\mu_B$ [6, 10, 12, 22]. It has been argued [22] that Ni atoms in CrNiAs, similarly to the case for the ferromagnetic ternary phosphides $(Cr_{1-x}Ni_x)_2P$ [27], carry no magnetic moment and that all the moment is carried by Cr atoms. On the other hand, electronic band structure calculations by Ishida *et al* [23] predict that $\mu_{Cr} = 1.19\ \mu_B$ and $\mu_{Ni} = 0.11\ \mu_B$ and those by Toboła *et al* [24] conclude that $\mu_{Cr} = 1.23\ \mu_B$ and $\mu_{Ni} = 0.12\ \mu_B$. Early neutron diffraction measurements of CrNiAs at 77 K suggested [12] that the Cr and Ni magnetic moments, $\mu_{Cr}$ and $\mu_{Ni}$, are coupled ferrimagnetically with $\mu_{Cr} = 0.55(15)\ \mu_B$ and $\mu_{Ni} = -0.65(15)\ \mu_B$. It was concluded from recent neutron diffraction measurements [25] that $\mu_{Cr} = 1.25(5)\ \mu_B$ and $\mu_{Ni} = 0.15(3)\ \mu_B$.

The above controversy concerning the Ni magnetic moment in CrNiAs can be resolved by using experimental techniques which probe this moment directly, such as rarely used $^{61}$Ni nuclear magnetic resonance (NMR) or $^{61}$Ni Mössbauer effect (ME). If there exists a magnetic moment on the Ni atoms in CrNiAs, the hyperfine magnetic field at $^{61}$Ni

[4] Author to whom any correspondence should be addressed.

 

nuclei determined from $^{61}$Ni NMR or $^{61}$Ni ME spectra must have a non-zero value. In this paper, we report on structural, magnetic, and $^{61}$Ni ME studies of the ternary arsenide CrNiAs.

## 2. Experimental procedure

A polycrystalline sample of CrNiAs was prepared from powders of Cr, Ni, and As with purities of 99.99%, 99.99%, and 99.999%, respectively. The powders were mixed in the desired proportion, sealed in an evacuated silica tube and annealed at 873 K for 2 days and then quenched. The reaction product was next subjected to a vacuum heat treatment at 1073 K for 2 days and then quenched. Finally, the ingot was pulverized, mixed well and heated again in vacuum at 1173 K for 7 days and then quenched.

X-ray diffraction measurements were performed at 298 K in Bragg–Brentano geometry on the PANanalytical X'Pert scanning diffractometer using Cu K$\alpha$ radiation. The K$\beta$ line was eliminated by using a Kevex PSi2 Peltier-cooled solid-state Si detector. In order to avoid the deviation from intensity linearity of the solid-state Si detector, its parameters and the parameters of the diffractometer were chosen in such a way as to limit the count rate from the most intense Bragg peaks to less than 9000 counts s$^{-1}$ [28].

The magnetic measurements were carried out with a Quantum Design superconducting quantum interference device magnetometer at various fields in the temperature range 5.0–300 K.

The $^{61}$Ni ME measurements were conducted using a standard Mössbauer spectrometer operating in sine mode, using the 67.4 keV transition in $^{61}$Ni [29, 30]. Both the source and the absorber were in direct contact with liquid helium in a cryostat. The spectrometer was calibrated with a 6.35 $\mu$m-thick $\alpha$-Fe foil [31], and the spectra were folded. The single line sources of $^{61}$Co (half life = 99 min) in $^{62}$Ni$_{0.85}$Cr$_{0.15}$ ($^{62}$Ni enriched to 97.7%) were activated in the MAinz MIcrotron (MAMI) using the nuclear reaction $^{62}$Ni $(\gamma, p)$ $^{61}$Co, with bremsstrahlung including the giant resonance region of 20–25 MeV necessary for this nuclear reaction to occur. A pneumatic tube approximately 50 m long was used to transport small platelets ($4 \times 4$ mm$^2$) of $^{62}$Ni$_{0.85}$Cr$_{0.15}$ to the activation position. Immediately after activation of about 2 h, the radioactive source material was pneumatically ejected and transported into a cryostat in which the Mössbauer absorber was already cooled to 4.2 K. Three sources had to be used to obtain a Mössbauer spectrum of sufficient signal-to-noise ratio. The Mössbauer absorber was made of pulverized material pressed into a teflon sample holder. The surface density of the Mössbauer absorber of the CrNiAs alloy was 839 mg cm$^{-2}$. The 67.4 keV $\gamma$-rays were detected with a 2.0 mm NaI(Tl) scintillation detector.

The measured $^{61}$Ni Mössbauer spectrum was analyzed by means of a least-squares fitting procedure which entailed calculations of the positions and relative intensities of the absorption lines by numerical diagonalization of the full hyperfine interaction Hamiltonian. In the principal axis system of the electric field gradient (EFG) tensor, the Hamiltonian can be written as [29, 30]

$$\hat{H} = g\mu_N H_{hf}\left[\hat{I}_z\cos\theta + \tfrac{1}{2}\left(\hat{I}_+ e^{-i\varphi} + \hat{I}_- e^{i\varphi}\right)\sin\theta\right] + \frac{eQV_{zz}}{4I(2I-1)}\left[3\hat{I}_z^2 - I(I+1) + \frac{\eta}{2}\left(\hat{I}_+^2 + \hat{I}_-^2\right)\right], \quad (1)$$

where $g$ is the nuclear $g$-factor of a nuclear state, $\mu_N$ is the nuclear Bohr magneton, $H_{hf}$ is the hyperfine magnetic field at a nuclear site, $e$ is the proton charge, $Q$ is the quadrupole moment of a nuclear state, $I$ is the nuclear spin, $V_{zz}$ is the $z$ component of the EFG tensor, $\eta$ is the asymmetry parameter defined as $\eta = |(V_{xx} - V_{yy})/V_{zz}|$ (if the principal axes are chosen such that $|V_{xx}| < |V_{yy}| < |V_{zz}|$, then $0 \leqslant \eta \leqslant 1$), $\theta$ is the angle between the direction of $H_{hf}$ and the $V_{zz}$-axis, $\varphi$ is the angle between the $V_{xx}$-axis and the projection of $H_{hf}$ onto the $xy$ plane, and the $\hat{I}_z$, $\hat{I}_+$, and $\hat{I}_-$ operators have their usual meaning. During the fitting procedure, the $g$ factors and the quadrupole moments for $^{61}$Ni ($I_g = 3/2$, $I_{ex} = 5/2$) were constrained to $g_{ex} = 0.1905$ and $g_g = -0.499\,87$, and $Q_{ex} = -0.196$ b and $Q_g = 0.162$ b, respectively [32].

The resonance line shape of the Mössbauer spectra was described by a transmission integral formula [33, 34]. In addition to the hyperfine parameters, only the absorber Debye–Waller factor $f_a$ and the absorber linewidth $\Gamma_a$ were fitted as independent parameters. The source linewidth $\Gamma_s = 0.440$ mm s$^{-1}$ and the background-corrected Debye–Waller factor of the source $f_s^* = 0.11$ [35], were used in the fit.

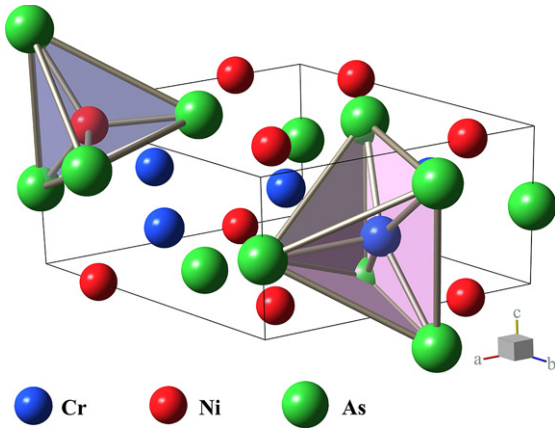


**Figure 1.** Crystal structure of CrNiAs. The pyramidal and tetrahedral coordinations of the Cr and Ni atoms are indicated.

## 3. Results and discussion

### 3.1. Structural characterization

The ternary arsenide CrNiAs crystallizes in the $Fe_2P$-type crystal structure with the space group $P\bar{6}2m$ (No. 189). In this structure type, the Cr and Ni atoms occupy, respectively, the 3g and 3f sites, whereas the As atoms occupy both the 1b and 2c sites. The unit cell contains four formula units of CrNiAs. The crystal structure of CrNiAs is shown in figure 1. The local surroundings of the Cr atoms are square pyramids of five As atoms, whereas the Ni atoms are located in tetrahedra of four As atoms.

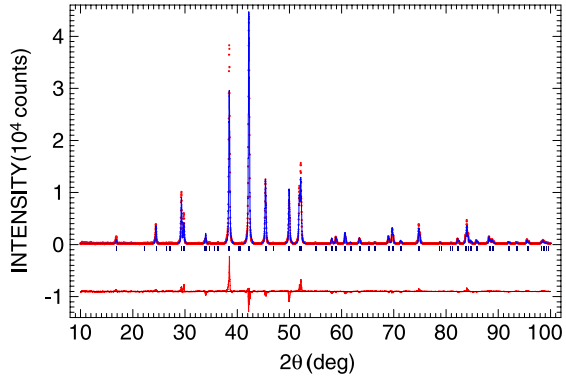


**Figure 2.** X-ray powder diffraction spectrum of CrNiAs at 298 K. The experimental data are denoted by open circles, while the line through the circles represents the results of the Rietveld refinement. The vertical bars represent the Bragg peak positions corresponding to the CrNiAs phase. The lower solid line represents the difference curve between experimental and calculated spectra.

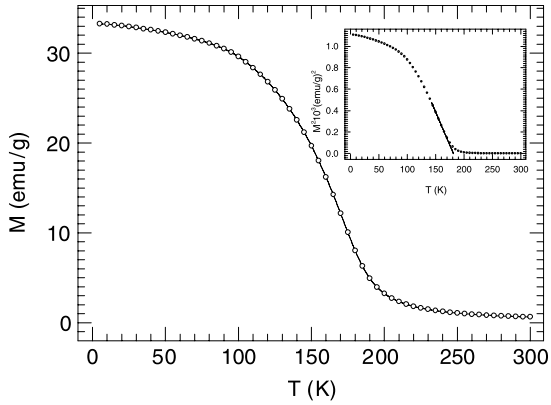


**Figure 3.** Temperature dependence of the magnetization of CrNiAs, measured in an external magnetic field of 10 kOe. The solid line is a guide for the eye. The inset shows the temperature dependence of the square of the magnetization and the solid line is a linear fit of the data around $T_C$.

**Table 1.** Atomic positions for the hexagonal arsenide CrNiAs obtained through Rietveld analysis.

| Atom | Site | Point symmetry | $x$ | $y$ | $z$ | Occupancy |
|---|---|---|---|---|---|---|
| Cr | 3g | $m2m$ | 0.5729(3) | 0 | $\frac{1}{2}$ | 1.0 |
| Ni | 3f | $m2m$ | 0.2515(2) | 0 | 0 | 1.0 |
| As1 | 1b | $\bar{6}2m$ | 0 | 0 | $\frac{1}{2}$ | 1.0 |
| As2 | 2c | $\bar{6}..$ | $\frac{1}{3}$ | $\frac{2}{3}$ | 0 | 1.0 |

The x-ray powder diffraction pattern of the sample studied is shown in figure 2. A Rietveld refinement of the x-ray powder diffraction data was performed yielding the lattice parameters $a = 6.1128(1)$ Å and $c = 3.6585(1)$ Å. The obtained atomic positions for the Cr and Ni sites are listed in table 1 and the interatomic distances are listed in table 2. The sample studied is single phase.

### *3.2. Magnetic properties*

The temperature dependence of the magnetization $M$ of CrNiAs measured in an applied magnetic field of 10 kOe between 5.0 and 300 K is shown in figure 3. This arsenide is obviously a ferromagnet. For a mean-field ferromagnet, $M^2 \propto T_C - T$ near $T_C$ [36]. From a linear fit of $M^2$ versus $T$ (inset in figure 3), $T_C$ was estimated to be 181.4(1.5) K.

The temperature dependence of the inverse magnetic susceptibility $\chi$ of CrNiAs is shown in figure 4. In the paramagnetic region the $\chi(T)$ data could be fitted to a modified Curie–Weiss law

$$\chi = \chi_0 + \frac{C}{T - \theta_p}, \qquad (2)$$

where $\chi_0$ is the temperature independent magnetic susceptibility, $C$ is the Curie constant, and $\theta_p$ is the paramagnetic Curie temperature. The Curie constant can be expressed as $C = \frac{N\mu_{eff}^2}{3k}$, where $N$ is the concentration of magnetic atoms per unit mass, $k$ is the Boltzmann constant, and $\mu_{eff}$ is the effective magnetic moment. The values of $\chi_0$, $C$, and $\theta_p$ obtained from the fit are $1.57(2.34) \times 10^{-7}$ emu Oe$^{-1}$ mol$^{-1}$, 1.461(6) emu Oe$^{-1}$ K mol$^{-1}$, and 176.0(3) K, respectively. This value of $C$ corresponds to $\mu_{eff}$ of 2.42(1) $\mu_B$ per transition-metal atom. The positive paramagnetic Curie temperature is consistent with the ferromagnetic ordering, and the value of $\theta_p$ is close to $T_C$.

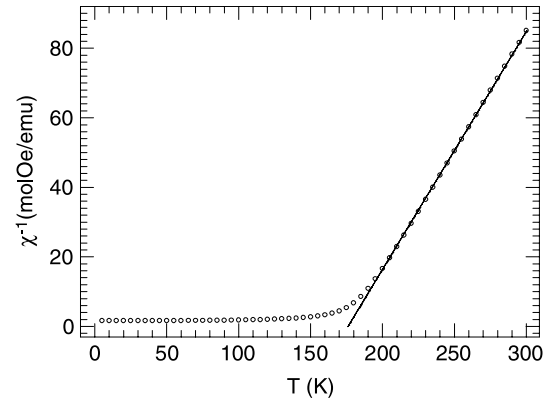


**Figure 4.** Temperature dependence of the inverse magnetic susceptibility of CrNiAs, measured in an external magnetic field of 10 kOe. The solid line is the fit to equation (2) in the temperature range 195–300 K.

Figure 5 shows a series of magnetization isotherms measured in the vicinity of $T_C$, estimated above. The usual procedure for extracting the spontaneous magnetization $M_S(T) = \lim_{H\to 0} M$, the inverse initial susceptibility $\chi_0^{-1} = \lim_{H\to 0}(H/M)$, and $T_C$ from the $M(H)$ isotherms is to make use of the Arrott plot [37], $M^2$ versus $H/M$. According to mean-field theory, near $T_C$ this plot should consist of a series of parallel lines for different temperatures, with the line at $T = T_C$ passing through the origin and $M_S(T)$ and $\chi_0^{-1}(T)$ are determined from the intercept values on the ordinate ($T \leqslant T_C$) and abscissa ($T \geqslant T_C$), respectively. Figure 6 shows the Arrott plot for CrNiAs. It consists of approximately parallel lines for fields larger than 6.0 kOe. The critical isotherm crossing the origin is found at 171.5(4) K.

**Table 2.** Interatomic distances (in Å) for the hexagonal arsenide CrNiAs.

| | | | | | | | | | | | |
|---|---|---|---|---|---|---|---|---|---|---|---|
| Cr | 4As | 2.580(1) | Ni | 2As | 2.328(1) | As1 | 6Ni | 2.389(1) | As2 | 3Ni | 2.328(1) |
| | 1As | 2.611(1) | | 2As | 2.389(1) | | 3Cr | 2.611(1) | | 6Cr | 2.580(1) |
| | 2Ni | 2.684(1) | | 2Ni | 2.663(1) | | | | | | |
| | 4Ni | 2.918(1) | | 2Cr | 2.684(1) | | | | | | |
| | 4Cr | 3.152(1) | | 4Cr | 2.918(1) | | | | | | |

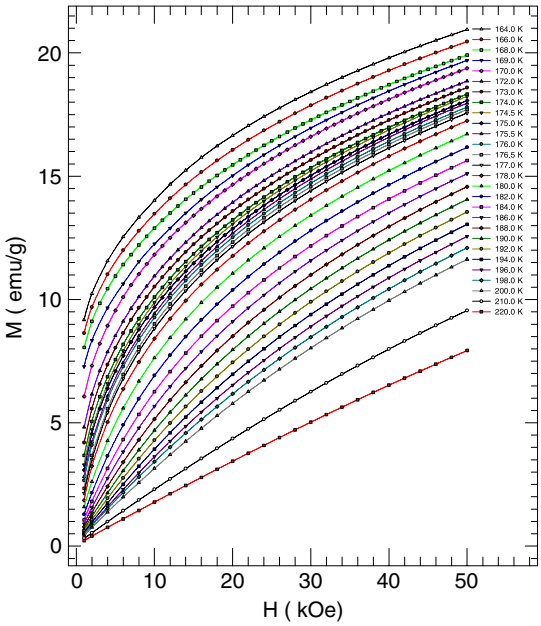


**Figure 5.** Magnetization isotherms versus magnetic field at temperatures between 164 and 220 K. The solid lines are guides for the eye.

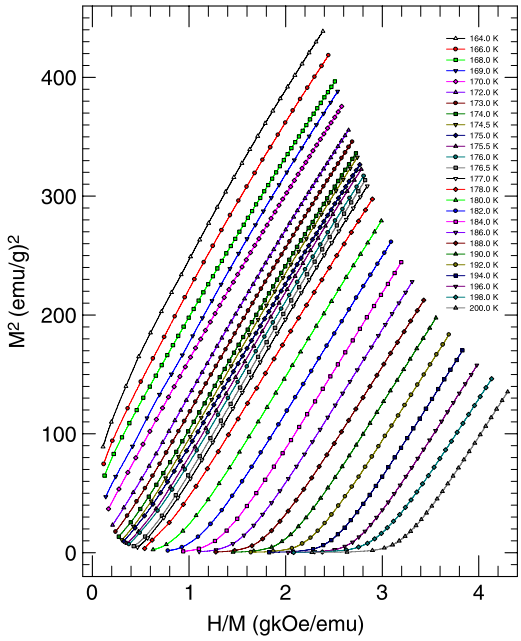


**Figure 6.** The Arrott plot for CrNiAs. The solid lines are guides for the eye.

According to the static scaling law equation, the second-order phase transition around $T_C$ is governed by a set of critical exponents $\beta$, $\gamma$, and $\delta$ through the relations [38]

$$M_S(T) = M_0(-\varepsilon)^{\beta}, \qquad \varepsilon < 0 \tag{3}$$

$$\chi_0^{-1}(T) = (h_0/M_0)\varepsilon^{\gamma}, \qquad \varepsilon > 0, \tag{4}$$

where $\varepsilon = (T - T_C)/T_C$, and $M_0$ and $h_0/M_0$ are the critical amplitudes. At $T_C$, a critical exponent $\delta$ relates $M$ and $H$ by [38]

$$M = DH^{1/\delta}, \qquad \varepsilon = 0, \tag{5}$$

where $D$ is a critical amplitude. Using the Arrott plot (figure 6), a linear extrapolation of the straight lines of the isotherms from fields above 6.0 kOe to $(M/H) = 0$ and $M = 0$ yields intercepts on the $M$ and $(M/H)$ axes, respectively, from which the values of $M_S(T)$ and $\chi_0^{-1}(T)$ are computed. These values as a function of temperature are plotted in figure 7. The fits of the $M_S(T)$ and $\chi_0^{-1}(T)$ data (figure 7) to equations (3) and (4) respectively give $\beta = 0.514(18)$, $T_C = 171.99(14)$ K and $\gamma = 1.010(16)$, $T_C = 171.83(6)$ K. The value of $T_C$ for CrNiAs is then taken as 171.9(1) K. The critical exponents obtained in this way are very close to those predicted by the mean-field theory ($\beta = 0.5$ and $\gamma = 1.0$).

To obtain the value of $\delta$, $M$ is plotted versus $H$ at 172.0 K in figure 8, the measured temperature closest to $T_C = 171.9(1)$ K. The fit of this isotherm to equation (5) (figure 8) gives $\delta = 2.922(10)$. This value is close to the value of $\delta = 3.0$ predicted by mean-field theory.

The critical exponents $\beta$, $\gamma$, and $\delta$ should fulfill the Widom exponent relation [39] $\gamma - \beta(\delta - 1) = 0$. The determined values of $\beta$, $\gamma$, and $\delta$ satisfy this relation well (0.022(56)), within experimental error.

The magnetic field dependence of the magnetization measured at 4.2 K is shown in figure 9. The magnetization does not saturate, even in a field of 50 kOe. The saturation magnetization at 4.2 K was obtained from the Arrott plot (inset in figure 9) by a linear extrapolation of the high-field data to $(M/H) = 0$. This yielded $M_S = 33.52(1.01)$ emu g$^{-1}$, which corresponds to the magnetic moment per formula unit $\mu_{FU} = 1.114(33)\ \mu_B$, or to the magnetic moment per transition metal (TM) atom (assuming that As atoms carry no magnetic moment) $\mu_{TM} = 0.557(17)\ \mu_B$.

### *3.3. Mössbauer spectroscopy*

Figure 10 shows a $^{61}$Ni Mössbauer spectrum of CrNiAs measured at 4.2 K. The Ni atoms are located in the crystal structure at a site with point symmetry $m2m$ (table 1). This ensures a non-zero electric field gradient at the Ni site and hence a possible non-zero electric quadrupole splitting. The spectrum in figure 10 clearly exhibits the presence of a poorly resolved hyperfine magnetic interaction. It was

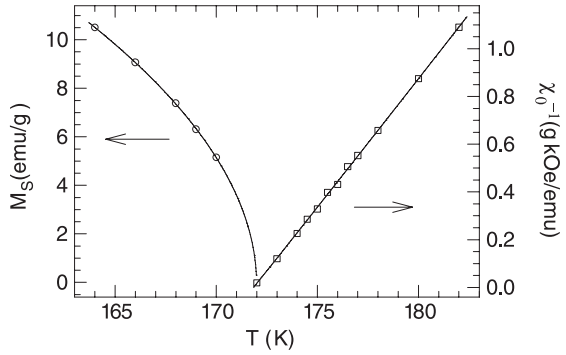


**Figure 7.** Temperature dependence of the spontaneous magnetization and the inverse initial susceptibility. The solid lines are fits of the experimental data to equations (3) and (4).

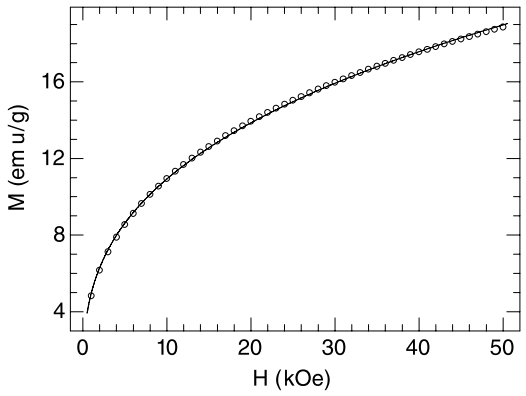


**Figure 8.** Magnetization isotherm versus magnetic field at 172.0 K. The solid line is the fit to equation (5).

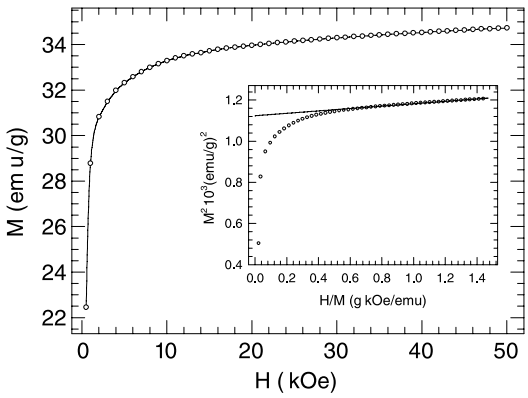


**Figure 9.** Magnetization isotherm versus magnetic field at 4.2 K. The solid line is a guide for the eye. The inset shows the Arrott plot. The solid line is a linear fit to the high-field data.

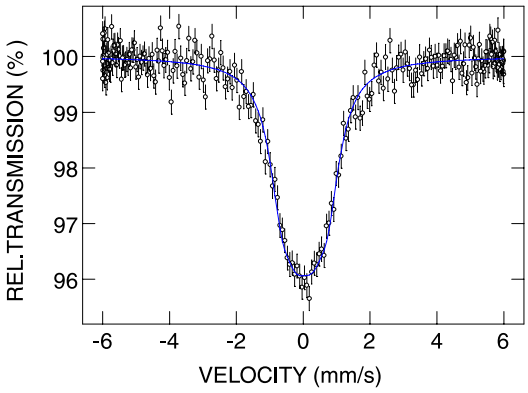


**Figure 10.** The $^{61}$Ni Mössbauer spectrum of CrNiAs measured at 4.2 K. The solid line is a fit, as described in the text. The zero-velocity origin is relative to the source.

fitted with the transmission integral by diagonalization of the hyperfine Hamiltonian (equation (1)). The following values of the hyperfine parameters were inferred from the fit: $\Gamma_a = 0.395(9)$ mm s$^{-1}$, the isomer shift (relative to the $^{61}$Co ($Ni_{0.85}Cr_{0.15}$) source) $\delta = 0.042(13)$ mm s$^{-1}$, $V_{zz} = -0.012(44) \times 10^{22}$ V m$^{-2}$, $f_a = 4.3(1)\%$, and $H_{hf} = 41.5(1.0)$ kOe.

The value of $\Gamma_a$ is only slightly larger than the natural linewidth $\Gamma_{nat} = 0.385$ mm s$^{-1}$ [32], as expected. Similarly to what has been found for other metallic systems [30, 40], the values of $\delta$ and $V_{zz}$ are essentially equal to zero. In terms of the Debye approximation for the lattice vibrations, the absorber Debye–Waller factor $f_a$ is expressed [29, 30] by the Debye temperature, $\Theta_D$, as

$$f_a(T) = \exp\left\{-\frac{3}{4}\frac{E_\gamma^2}{Mc^2k\Theta_D}\left[1+\left(\frac{T}{\Theta_D}\right)^2\int_0^{\Theta_D/T}\frac{x\,dx}{e^x-1}\right]\right\}, \quad (6)$$

where $E_\gamma$ is the energy of the Mössbauer transition, $M$ is the mass of the Mössbauer nucleus, $c$ is the speed of light, and $k$ is the Boltzmann constant. The value of $f_a$ obtained from the fit via equation (6) yields $\Theta_D = 221(1)$ K.

A non-zero value of $H_{hf}$ implies a non-zero value of the nickel magnetic moment $\mu_{Ni}$ in CrNiAs. There is no firmly established relationship between the measured $H_{hf}$ and $\mu_{Ni}$. There are two major contributions to $H_{hf}$ at the nuclei of TM elements in metallic alloys [29, 30]: the core contribution, due to the polarization of core s electrons and the polarization of the conduction electrons by the 3d electrons (i.e., by the on-site magnetic moment), and the conduction electron contribution, due to the polarization of the conduction electrons by the surrounding magnetic moments. The first contribution is proportional to the local magnetic moment $\mu_l$, whereas the second contribution is assumed to be proportional to the average moment per magnetic atom $\mu_{TM}$ Thus, a phenomenological relation is used [41]

$$H_{hf} = a\mu_l + b\mu_{TM}, \quad (7)$$

where $a$ and $b$ are assumed to be constant for a given alloy system. This relation enables one to estimate the value of $\mu_l$ from the measured values of $H_{hf}$ and $\mu_{TM}$, provided that the values of $a$ and $b$ are known from an earlier calibration. Due to the scarcity of data on the values of $H_{hf}$ at $^{61}$Ni nuclei in Ni-containing alloys, the values of $a$ and $b$ are known only for a few alloy series [42–46]. For the ternary pnictides Cr–Ni–X (X = metalloid), $a = 63$ kOe/$\mu_B$ and $b = 57$ kOe/$\mu_B$ [47]. Using the value of $\mu_{TM}$ determined above and the measured value of $H_{hf}$, one obtains $\mu_{Ni} = 0.15(3)$ $\mu_B$

from equation (7). It is thus concluded that the Ni atoms in the CrNiAs ferromagnet do carry a magnetic moment. This finding is at variance with the theoretical prediction of $\mu_{Ni} = 0$ in CrNiAs [22, 27] and in agreement with the prediction based on the electronic structure calculations of the non-zero $\mu_{Ni}$ in CrNiAs [23, 24]. Since the Ni and Cr magnetic moments are coupled ferromagnetically in CrNiAs, the values of $\mu_{Ni} = 0.15(3)\ \mu_B$ and $\mu_{FU} = 1.114(33)\ \mu_B$ imply that the Cr atoms carry a magnetic moment of $0.95(6)\ \mu_B$.

## 4. Conclusions

The ternary arsenide CrNiAs has been studied by means of x-ray diffraction, magnetization measurements, and $^{61}$Ni Mössbauer spectroscopy. The studied compound has the hexagonal $Fe_2P$-type structure (space group $P\bar{6}2m$) with the lattice parameters $a = 6.1128(1)$ Å and $c = 3.6585(1)$ Å. The Curie temperature $T_C$ is found to be 171.9(1) K and three critical exponents are determined $\beta = 0.514(18)$, $\gamma = 1.010(16)$, and $\delta = 2.922(10)$. The values of these critical exponents are close to those of a mean-field ferromagnet. The temperature dependence of the magnetic susceptibility above $T_C$ follows the modified Curie–Weiss law with a paramagnetic Curie temperature 176.0(3) K and an effective magnetic moment per transition metal atom $2.42(1)\ \mu_B$. The magnetic moment per formula unit at 4.2 K is found to be $1.114(33)\ \mu_B$. The hyperfine magnetic field of 41.5(1.0) kOe at $^{61}$Ni nuclei at 4.2 K implies that the Ni atoms carry a magnetic moment of $0.15(3)\ \mu_B$, and that the moment carried by the Cr atoms is $0.95(6)\ \mu_B$. The Debye temperature of CrNiAs is 221(3) K.

## Acknowledgment

This work was supported by the Natural Sciences and Engineering Research Council of Canada.

## References

[1] Hollan A 1966 *Ann. Chim. Fr.* **1** 437
[2] Nylund A, Roger A, Senateur J P and Fruchart R 1971 *Monatsh. Chem.* **102** 1631
[3] Roy-Montreuil M, Deyris B, Michel A, Rouault A, L'Héritier P, Nylund A, Sénateur J P and Fruchart R 1971 *Mater. Res. Bull.* **7** 813
[4] Nylund A, Roger A, Sénateur J P and Fruchart R 1972 *J. Solid State Chem.* **4** 115
[5] Jognson V 1973 *Mater. Res. Bull.* **8** 1067
[6] Krumbügel-Nylund A, Sénateur J P, Boursier D and Fruchart R 1974 *C. R. Acad. Sci. Paris* C **278** 85
[7] Senateur J P, Rouault A, Fruchart R, Capponi J J and Perroux M 1976 *Mater. Res. Bull.* **11** 631
[8] Guérin R and Sergent M 1977 *Mater. Res. Bull.* **12** 381
[9] Sénateur J P, Fruchart D, Boursier D, Rouault A, Montreuil J R and Deyris B 1977 *J. Physique Coll.* **12** C7 61
[10] Iwata N, Matsushima T, Fujii H and Okamoto T 1980 *J. Phys. Soc. Japan* **49** 1318
[11] Fruchart R 1982 *Ann. Chim. Fr.* **7** 563
[12] Fruchart D, Fruchart R and Sénateur J P 1982 *Proc. VII Int. Conf. on Solid Comp. Trans. Elem. (Grenoble)* p IIIA1
[13] Backmann M and Fruchart D 1982 *Proc. VII Int. Conf. on Solid Comp. Trans. Elem. (Grenoble)* p IIIA2
[14] Chaudouët P, Montreuil J R, Senateur J P, Boursier D, Rouault A and Fruchart R 1982 *Proc. VII Int. Conf. on Solid Comp. Trans. Elem. (Grenoble)* p IIIA4
[15] Meisner G P, Ku H C and Barz H 1983 *Mater. Res. Bull.* **18** 983
[16] Chenevier B, Fruchart D, Backmann M, Senateur J P, Chaudouet P and Lundgren L 1984 *Phys. Status Solidi* a **84** 199
[17] Backmann M, Chenevier B, Fruchart D, Laborder O and Soubeyroux J L 1986 *J. Magn. Magn. Mater.* **54–57** 1541
[18] Bartolomé J, Garcia J, Floría L M, Falo F, Navarro R, Fruchart D, Backmann M and de Jongh L J 1986 *J. Magn. Magn. Mater.* **54–57** 1547
[19] Kanomata T, Shirakawa K, Yasui H and Kaneko T 1987 *J. Magn. Magn. Mater.* **68** 286
[20] Chenevier B, Laborder O, Backmann M, Fruchart D, Fruchart R and Puertolas J A 1988 *J. Phys. F: Met. Phys.* **18** 1867
[21] Kanomata T, Kawashima T, Utsugi H, Goto T, Hasegawa H and Kaneko T 1991 *J. Appl. Phys.* **69** 4639
[22] Ohta S, Kaneko T, Yoshida H, Kanomata T and Yamauchi H 1995 *J. Magn. Magn. Mater.* **150** 157
[23] Ishida S, Takiguchi T, Fujii S and Asano S 1996 *Physica* B **217** 87
[24] Toboła J, Kaprzyk S, Fruchart D, Bacmann M, Wolfers P and Fruchart R 1997 *J. Alloys Compounds* **262/263** 65
[25] Bacmann M, Fruchart D, Koumina A and Wolfers P 2004 *Mater. Sci. Forum* **443/444** 379
[26] Fruchart D, Allab F, Balli M, Gignoux D, Hlil E K, Koumina A, Skryabina N, Tobola J, Wolfers P and Zach R 2005 *Physica* A **358** 123
[27] Goodenough J B 1973 *J. Solid State Chem.* **7** 428
[28] Bish D L and Chipera S J 1989 *Powder Diffract.* **4** 137
[29] Greenwood N N and Gibb T C 1971 *Mössbauer Spectroscopy* (London: Chapman and Hall)
[30] Gütlich P, Link R and Trautwein A 1978 *Mössbauer Spectroscopy and Transition Metal Chemistry* (Berlin: Springer)
[31] Cali J P (ed) 1971 *Certificate of Calibration, Iron Foil Mössbauer Standard* (Washington, DC: US Government Printing Office) NBS (US) Circular No. 1541
[32] Stevens J G 1981 *CRC Handbook of Spectroscopy* vol 3, ed J W Robinson (Boca Raton, FL: CRC Press) p 403
[33] Margulies S and Ehrman J R 1961 *Nucl. Instrum. Methods* **12** 131
[34] Shenoy G K, Friedt J M, Maletta H and Ruby S L 1974 *Mössbauer Effect Methodology* vol 10, ed I J Gruverman, C W Seidel and D K Dieterly (New York: Plenum) p 277
[35] Rummel H 1982 $^{61}$Ni-Mössbauer-Untersuchungen der Magnetischen Hyperfeinfelder in Nickelspinellen *PhD Thesis* Johannes Gutenberg-Universität Mainz
[36] Zijlstra H 1967 *Experimental Methods in Magnetism* vol 2 (Amsterdam: North-Holland)
[37] Arrott A 1957 *Phys. Rev.* **108** 1394
[38] Stanley H E 1971 *Introduction to Phase Transitions and Critical Phenomena* (New York: Oxford University Press)
[39] Widom B 1964 *J. Chem. Phys.* **41** 1633
Widom B 1965 *J. Chem. Phys.* **43** 3898
[40] Tomala K, Czjzek G, Fink J and Schmidt H 1977 *Solid State Commun.* **24** 857
[41] Johnson C E, Ridout M S and Cranshaw T E 1963 *Proc. Phys. Soc.* **81** 1079
Collins M F and Wheeler D A 1963 *Proc. Phys. Soc.* **82** 633
Panissod P, Durand J and Budnick J I 1982 *Nucl. Instrum. Methods* **199** 99

Panissod P 1985 *Hyperfine Interact.* **124–126** 607
[42] Erich U 1969 *Z. Phys.* **227** 25
Ebert H, Winter H, Gyorffy B L, Johnson D D and Pinski F J 1988 *J. Phys. F: Met. Phys.* **18** 719
[43] Stadnik Z M, Griesbach P, Dehe G, Gütlich P and Maniawski F 1987 *J. Magn. Magn. Mater.* **70** 436
[44] Tansil J E, Obenshain F E and Czjzek G 1972 *Phys. Rev.* B **6** 2796
[45] Streever R L and Uriano G A 1966 *Phys. Rev.* **149** 295
[46] Stadnik Z M, Griesbach P, Dehe G, Gütlich P, Stroink G and Miyazaki T 1987 *Phys. Rev.* B **35** 8740
[47] Stadnik Z M, Wang P, Jansen N, Walcher D, Gütlich P and Kanomata T 2008 unpublished results